Electronic Supplementary Material (ESI) for Physical Chemistry Chemical Physics.

Triplet-triplet annihilation upconversion followed by FRET for the red light activation of a photodissociative ruthenium complex in liposomes

Sven H. C. Askes[a], Miroslav Kloz[b], Gilles Bruylants[c], John Kennis[b], and Sylvestre Bonnet[a]

[a] Leiden Institute of Chemistry, Gorlaeus Laboratories, Leiden University, P.O. Box 9502, 2300 RA Leiden, The Netherlands; [b] Laserlab Amsterdam, VU University Amsterdam, De Boelelaan 1081, 1081 HV Amsterdam, The Netherlands; [c] Engineering of Molecular NanoSystems, Université Libre de Bruxelles, 50 av. F.D. Roosevelt, 1050 Brussels, Belgium.

SUPPLEMENTARY INFORMATION

Table of contents

1. Ru concentration in liposome samples by inductively coupled plasma optical emission spectroscopy

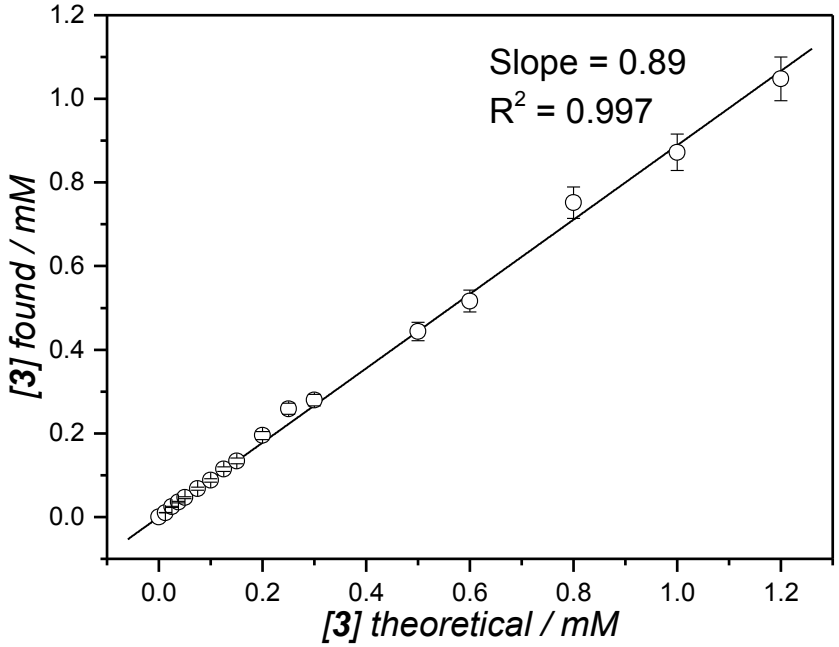

Figure S1. Bulk concentrations of 3^{2+} experimentally found in PEGylated DMPC liposome samples, determined by inductively coupled plasma optical emission spectroscopy, versus theoretical concentrations. As best fit, a straight line was plotted through the origin with a slope of 0.89 (R^2 = 0.997). Error bars represent 5% instrumental error.

The bulk concentration of $\mathbf{3}^{2+}$ in liposome samples was measured with inductively coupled plasma optical emission spectroscopy (ICP-OES), see Figure S1. From the slope of a linear fit of the measured values plotted versus theoretical values it was determined that on average, 89% of the theoretical concentration $\mathbf{3}^{2+}$ was experimentally found. In all experiments when the determined value was too low with respect to the threshold of the ICP-OES machine, an extrapolated value was used from the theoretical concentration multiplied by 0.89.

2. Differential scanning calorimetry

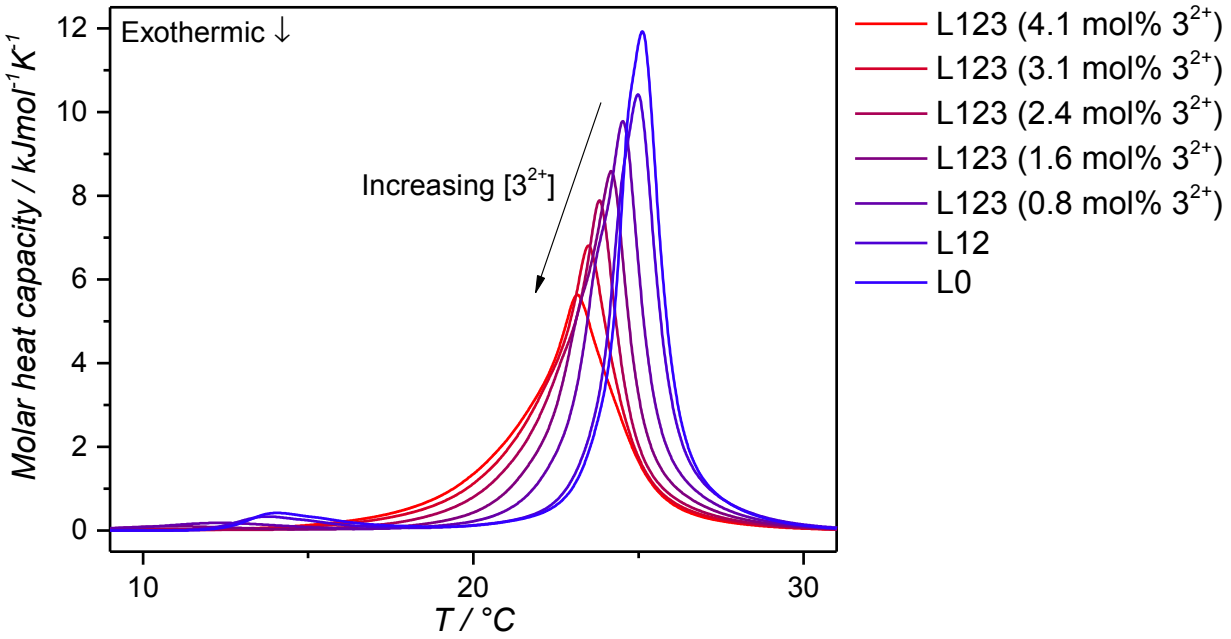

Figure S2. Differential scanning calorimetry thermograms (in heating mode) for PEGylated (4 mol%) DMPC liposomes without any chromophores (L0), with the TTA-UC dye couple (L12), and with the TTA-UC dye couple and various amounts of 3^{2+} added (L123). Reported molar percentages of 3^{2+} are based on ICP-OES measurements (see main text). Measurements were performed with a scanning rate of 1 K.min^{-1} at 3 atm. pressure.

Table S1. Differential scanning calorimetry data for PEGylated (4 mol%) DMPC liposomes without any chromophores (L0), with the TTA-UC dye couple (L12), and with the TTA-UC dye couple and various amounts of 3^{2+} added (L123) , with T_m (in °C) as the main transition temperature and ΔH (in kJ.mol^{-1}) as the molar change in enthalpy when heating from 10 to 35 °C. Reported molar percentages of 3^{2+} are based on ICP-OES measurements (see main text). Measurements were performed with a scanning rate of 1 K.min^{-1} at 3 atm. pressure.

Sample	3^{2+} molar percentage	T_m (°C)	ΔH (kJ.mol^{-1})
L0	-	25.1	25.1
L12	-	25.0	23.1
L123	0.8	24.5	23.8
L123	1.6	24.2	22.4
L123	2.4	23.8	21.6
L123	3.1	23.5	21.7
L123	4.1	23.2	21.1

3. Photodissociation experiments using red light

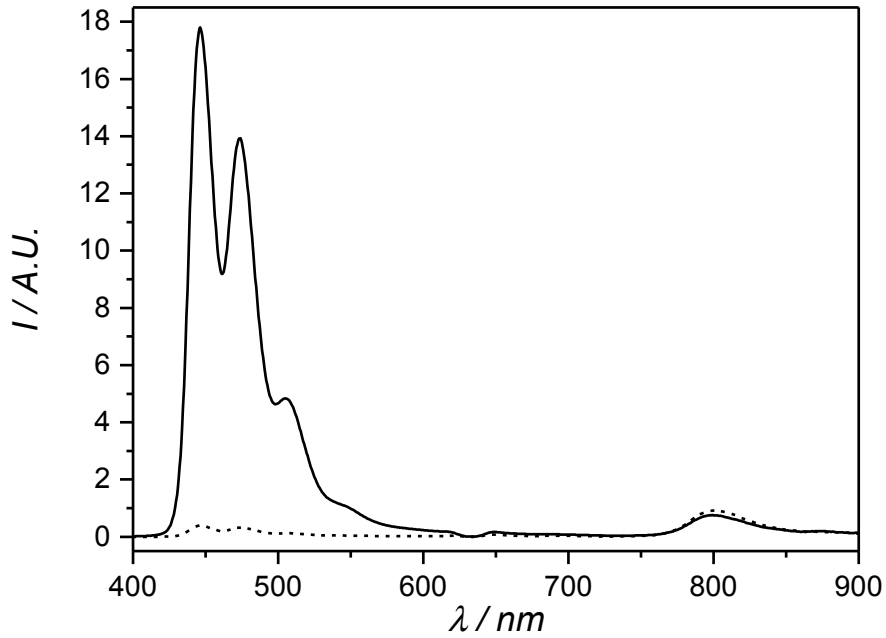

Figure S3. Luminescence emission spectrum of L12 (black) and L123 with 3.3 mol% 3^{2+} at t = 0 of the irradiation experiment using red light (dashed). λ_{exc} = 630 nm. Irradiation conditions: power 120 mW, beam diameter 4 mm, intensity 0.95 Wcm^{-2}, T = 310 K, sample volume 1.5 ml. The liposome dispersion was diluted prior to measurement so that [2] = 2.5 μM and [1] = 0.25 μM, and in the case of L123, the concentration of 3^{2+} = 18 μM.

4. Lifetime studies with time-correlated single photon counting and transient absorption spectroscopy

4.1. Analysis of time-correlated single photon counting data

Fluorescence lifetime measurements were performed using time-correlated single photon counting (TCSPC). The obtained histograms were fitted with Origin Pro software as the sum of single exponential decays, as described by Equation S1:

$$I(t) = \sum_i A_i e^{\frac{t}{\tau_i}} \qquad \textbf{Equation S1}$$

where t is time, I(t) is the time-dependent observed emission intensity (photon counts), A_i is the decay amplitude, and τ_i is the decay constant. For each sample, fitting with a single exponential decay curve did not give satisfactory fits. In the case of liposomes **L2**, this is attributed to the molecules being dissolved in a heterogeneous system (e.g. liposomes), and a small degree of self-energy transfer (homo-transfer) due to clustering of **2** in the membrane.[1] In the case of **L23** or **L123**, the occurrence of energy transfer results in a multitude of donor excited state lifetimes, i.e. multi-exponential decays. To achieve a single lifetime value, required for further data processing, it was therefore necessary to use amplitude weighted average lifetimes (τ), as calculated by Equation S2:

$$\tau = \frac{\sum_i A_i \tau_i}{\sum_i A_i} \qquad \textbf{Equation S2}$$

4.2. Time-correlated single photon counting data

Table S2. Fitting parameters to various decay functions for the fluorescence lifetime (in ns) of compound 2, as measured with TCSPC at 293 K (λ_{exc} = 440 nm, and λ_{emi} = 474 nm), in PEGylated DMPC liposomes with a fixed amount (0.5 mol%) of 2 while varying the molar percentage of 3^{2+} from 0 to 6%, as well as the calculated parameters τ as the amplitude averaged lifetime calculated from τ_1, A_1, τ_2, A_2, τ_3, and A_3 by Equation S2, and E_{ET} as the efficiency of energy transfer calculated from Equation S6. Goodness of fit expressed as R^2 values. The bulk concentration of 3^{2+} was determined by ICP-OES. Bulk concentration of DMPC, DSPE-PEG-2000, and compound 2 were 0.20 mM, 8 µM, and 1 µM, respectively.

Decay function	Concentration of 3^{2+} in the membrane in mol%										
	0.0%	0.2%	0.5%	0.7%	0.9%	1.7%	2.1%	2.4%	3.5%	5.0%	5.6%
Multi-exponential											
τ_1 (A_1 in %)	6.49 ± 0.01 (93.4%)	5.82 ± 0.01 (76.7%)	5.37 ± 0.01 (82.9%)	5.10 ± 0.13 (43.8%)	4.56 ± 0.08 (35.6%)	2.43 ± 0.03 (37.1%)	2.85 ± 0.08 (21.3%)	3.35 ± 0.19 (18.2%)	2.12 ± 0.18 (19.3%)		
τ_2 (A_2 in %)	1.58 ± 0.06 (6.6%)	1.64 ± 0.02 (23.3%)	1.30 ± 0.02 (17.1%)	2.09 ± 0.16 (37.6%)	1.79 ± 0.08 (41.7%)	0.79 ± 0.05 (40.3%)	0.98 ± 0.06 (42.3%)	1.21 ± 0.08 (40.7%)	0.85 ± 0.14 (33.2%)	1.20 ± 0.01 (24.1%)	0.96 ± 0.01 (41.3%)
τ_3 (A_3 in %)				0.63 ± 0.04 (18.6%)	0.54 ± 0.03 (22.7%)	0.30 ± 0.03 (22.6%)	0.32 ± 0.02 (36.4%)	0.37 ± 0.01 (41.1%)	0.33 ± 0.02 (47.5%)	0.31 ± 0.00 (75.9%)	0.29 ± 0.01 (58.7%)
τ	6.17 ± 0.01	4.85 ± 0.01	4.67 ± 0.01	3.14 ± 0.08	2.50 ± 0.05	1.29 ± 0.02	1.14 ± 0.03	1.25 ± 0.05	0.85 ± 0.06	0.53 ± 0.00	0.57 ± 0.01
R^2	0.9997	0.9996	0.9996	0.9996	0.9995	0.9994	0.9992	0.9993	0.9992	0.9991	0.9992
E_{ET}	0%	21.4%	24.2%	49.1%	59.5%	79.1%	81.5%	79.7%	86.2%	91.4%	90.8%
Förster 3D model											
γ	0.00 ± 0.00	0.23 ± 0.00	0.28 ± 0.00	0.74 ± 0.01	1.044 ± 0.01	1.82 ± 0.01	2.04 ± 0.01	1.93 ± 0.01	2.67 ± 0.02	3.99 ± 0.08	3.84 ± 0.08
R^2	0.9995	0.9996	0.9996	0.9995	0.9995	0.9994	0.9992	0.9993	0.9991	0.9991	0.9991

Table S3. Fitting parameters to various decay functions for the fluorescence lifetime (in ns) of compound 2, as measured with TCSPC at 310 K (λ_{exc} = 440 nm, and λ_{emi} = 474 nm), in PEGylated DMPC liposomes with a fixed amount (0.5 mol%) of 2 while varying the molar percentage of 3^{2+} from 0 to 6%, as well as the calculated parameters τ as the amplitude averaged lifetime calculated from τ_1, A_1, τ_2, A_2, τ_3, and A_3 by Equation S2, and E_{ET} as the efficiency of energy transfer calculated from Equation S6. Goodness of fit expressed as R^2 values. The bulk concentration of 3^{2+} was determined by ICP-OES. Bulk concentration of DMPC, DSPE-PEG-2000, and compound 2 were 0.20 mM, 8 μM, and 1 μM, respectively.

Decay function	Concentration of 3^{2+} in the membrane in mol%										
	0.0%	0.2%	0.5%	0.7%	0.9%	1.7%	2.1%	2.4%	3.5%	5.0%	5.6%
Multi-exponential											
τ_1 (A_1 in %)	5.94 ± 0.01 (93.8%)	5.33 ± 0.01 (79.7%)	4.79 ± 0.01 (77.1%)	4.01 ± 0.03 (62.9%)	4.06 ± 0.11 (35.8%)		2.61 ± 0.20 (7.0%)				
τ_2 (A_2 in %)	2.01 ± 0.10 (6.2%)	1.72 ± 0.03 (20.3%)	1.35 ± 0.02 (22.9%)	1.38 ± 0.10 (28.6%)	1.86 ± 0.13 (41.4%)	1.85 ± 0.01 (45.4%)	1.07 ± 0.08 (31.8%)	1.53 ± 0.01 (37.8%)	0.84 ± 0.01 (28.9%)	0.66 ± 0.01 (12.9%)	0.72 ± 0.01 (17.4%)
τ_3 (A_3 in %)				0.49 ± 0.09 (8.5%)	0.64 ± 0.03 (22.7%)	0.54 ± 0.00 (54.6%)	0.40 ± 0.02 (61.2%)	0.43 ± 0.00 (62.2%)	0.30 ± 0.00 (71.1%)	0.23 ± 0.00 (87.1%)	0.26 ± 0.00 (82.6%)
τ	5.69 ± 0.01	4.60 ± 0.01	4.00 ± 0.01	2.96 ± 0.03	2.37 ± 0.07	1.14 ± 0.00	0.77 ± 0.03	0.84 ± 0.00	0.45 ± 0.00	0.29 ± 0.00	0.34 ± 0.00
R^2	0.9997	0.9997	0.9996	0.9996	0.9996	0.9995	0.9993	0.9993	0.9994	0.9985	0.9990
E_{ET}	0%	19.2%	29.7%	52%	58.3%	80.0%	86.5%	85.2%	92.1%	95.1%	94.0%
Förster 3D model											
γ	0.00 ± 0.01	0.22 ± 0.00	0.36 ± 0.00	0.74 ± 0.01	1.15 ± 0.01	2.25 ± 0.02	2.86 ± 0.02	2.75 ± 0.01	5.49 ± 0.09	8.46 ± 0.19	7.25 ± 0.14
R^2	0.9996	0.9997	0.9996	0.9996	0.9996	0.9994	0.9993	0.9992	0.9993	0.9982	0.9989

4.3. Analysis of transient absorption data

Data from transient absorption (TA) spectroscopy was fitted using the software package Glotaran, with which the user can conveniently analyse TA data and correct for experimental artefacts. The software features global fitting, with which different components that contribute to the data can be untangled and represented as separate datasets.[2] Each component i in the observed time-dependent transient absorption spectrum ΔOD(t,λ) is described with a non-normalized Decay Associated transient absorption Spectrum $DAS_i(\lambda)$ and a single exponential decay function with decay constant τ_i, see Equation S3:

$$\Delta OD(t,\lambda) = \sum_i DAS_i(\lambda) * e^{\frac{t}{\tau_i}} \qquad \textbf{Equation S3}$$

In the case of multi-exponential behaviour of one of the species (i.e. **2** in presence of $\mathbf{3}^{2+}$), multiple components were identified with different τ_i, but with identical $DAS_i(\lambda)$. The amplitude averaged lifetime (τ) was then calculated using Equation S4:

$$\tau = \frac{\sum_i B_i \tau_i}{\sum_i B_i} \qquad \textbf{Equation S4}$$

in which B_i represents the relative amplitude of DAS_i. For measurements on liposomes **L2** and **L23**, i.e. experiments that were meant to probe the lifetime of **2**, B_i was calculated from the average DAS value at 695 – 705 nm, at which **2** has a very strong transient peak, while the influence of $\mathbf{3}^{2+}$ is negligible (see below). For measurements on liposomes with only $\mathbf{3}^{2+}$ (i.e. **L3** liposomes), A_i was calculated from the average DAS value from 445 – 455 nm, where the transient absorption of $\mathbf{3}^{2+}$ is strongest (see below).

4.4. Transient absorption data

Table S4. Fitting parameters to various decay functions for the excited state lifetime (in ns) of compound 2, as measured with TA spectroscopy at 293 K (λ_{exc} = 400 nm), in PEGylated DMPC liposomes with a fixed amount (0.5 mol%) of 2 while varying the molar percentage of 3^{2+} from 0 to 3%, as well as the calculated parameters τ as the amplitude averaged lifetime calculated from τ_3, B_3, τ_4, and B_4 by Equation S4, and E_{ET} as the efficiency of energy transfer calculated from Equation S6. Goodness of fit expressed as R^2 values. Bulk concentration of DMPC, DSPE-PEG-2000, and compound 2 were 20 mM, 0.8 mM, and 0.1 mM, respectively. All experimental details can be found in the experimental section.

Kinetic model				**3^{2+} mol%**		
	0	0.4%	0.8%	1.7%	2.5%	3.3%
Multi-exponential (GLOTARAN)						
τ_1	0.10E-3 ± 0.00E-3	0.01E-3 ± 0.00E-3	0.11E-3 ± 0.00E-3	0.02E-3 ± 0.00E-3	0.09E-3 ± 0.00E-3	0.07E-3 ± 0.00E-3
τ_2	8.3E-3 ± 0.1E-3	8.9E-3 ± 0.09E-3	9.2E-3 ± 0.13E-3	9.1E-3 ± 0.14E3	9.9E-3 ± 0.17E-3	5.5E-3 ± 0.11E-3
τ_3 (B_3 in %)	2.30 ± 0.12 (22.1%)	0.45 ± 0.00 (27.0%)	0.26 ± 0.00 (41.7%)	0.19 ± 0.00 (49.1%)	0.11 ± 0.00 (57.6%)	0.07 ± 0.00 (55.3%)
τ_4 (B_4 in %)	7.05 ± 0.12 (77.9%)	3.99 ± 0.02 (73.0%)	2.43 ± 0.01 (58.3%)	1.85 ± 0.01 (50.1%)	0.79 ± 0.01 (42.4%)	0.56 ± 0.00 (44.7%)
τ_5	118 ± 34	629 ± 78	916 ± 161	6380 ± 4160	1850 ± 359	613 ± 79
τ	6.00 ± 0.10	3.03 ± 0.02	1.52 ± 0.01	1.04 ± 0.01	0.40 ± 0.00	0.29 ± 0.00
E_{ET}	0%	49.5%	74.7%	82.7%	93.3%	95.1%
Förster 3D model						
γ	0.02 ± 0.02	0.43 ± 0.02	1.00 ± 0.06	1.35 ± 0.05	2.43 ± 0.07	2.99 ± 0.09
R^2	0.9974	0.9991	0.9959	0.9975	0.9968	0.9969

4.5. Transient absorption in liposomes L2

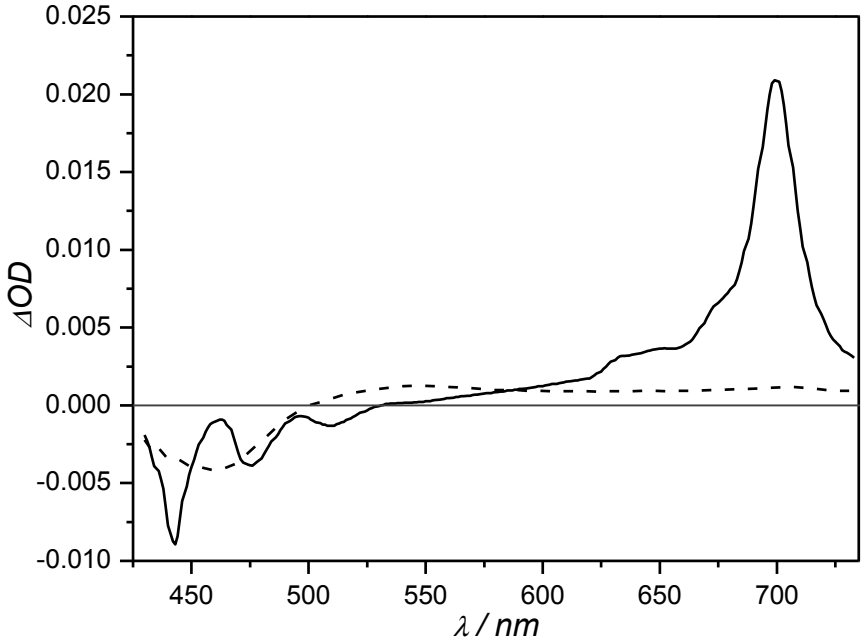

Figure S4. Transient absorption spectra at 293 K of PEGylated DMPC liposomes with either 0.5 mol% 2 (liposomes L2, solid line), 1.0 ns after the excitation pulse, and 3.3 mol% 3^{2+} (liposomes L3, dashed line), 1.0 ps after the excitation pulse. Both samples were excited with 400 nm light (20-60 nJ/pulse, 1 kHz repetition rate). Bulk DMPC concentration: 20 mM.

The transient absorption spectrum of PEGylated DMPC liposomes bearing 0.5 mol% **2** (liposomes **L2**), 1.0 ns after a 400 nm excitation pulse, is displayed in Figure S4. The spectrum closely matches literature reports for perylene in cyclohexane, and features negative signals from 430 to 550 nm, due to ground state bleach and stimulated emission, and a strong positive band centred at 700 nm, due to excited state absorption as the result of an S_1-S_n transition.[3] The transient absorption data was analysed with Glotaran and was best-fitted using 5 single-exponential decay functions (Table S4). The fastest decay component (τ_1 = 0.1 ps) is attributed to coherent artefacts due to spatial and temporal overlap of the pump and probe pulses around t = 0. The second decay component (τ_2 = 8.3 ps) is attributed to vibrational relaxation of compound **2** and/or solvent relaxation of the phospholipid matrix. A component with a very long lifetime (τ_5 > 100 ns) and almost negligible amplitude is attributed to either triplet state and/or excimer absorption. The nanosecond scale components with τ_3 = 2.3 and τ_4 = 7.1 ns have identical spectra, which indicates that they originate from the same species. In this case, τ_1, τ_2, and τ_5 were not taken into account for calculating τ by Equation S4, so that $\tau = \tau_{34}$ = 6.00 ± 0.10 ns, which corresponds to literature values of the excited state lifetime of **2**.[1, 3]

4.6. Transient absorption in liposomes L3

Next, the transient absorption of liposomes with 3.3 mol% of $\mathbf{3}^{2+}$ (liposomes **L3**) was evaluated. It was confirmed with UV-VIS spectroscopy before and after the experiment that negligible photodissociation occurred during the time-resolved spectroscopic analysis. The maximum amount of photodissociation, expressed as the total amount of mol $\mathbf{4}^{2+}$, can be estimated from the photon flux at 400 nm (Φ_{400} = 30 µW, i.e. = 1.0 x 10^{-10} einstein.s^{-1}), measurement time (≤ 7200 s), quantum yield of photodissociation (0.52%),[4] and chance of absorption (A_{400} ≤ 0.60), see Equation S5:

$$n_{\mathbf{4}} = (1 - 10^{-A})\Phi_{400}\Phi_{Ru}t \qquad \textbf{Equation S5}$$

The value of $n_{\mathbf{4}}$ for these experiments is ≤ 2.8 x 10^{-9} mol. With a sample volume of 200 µL and a $\mathbf{3}^{2+}$ concentration of 0.71 mM (as determined by ICP-OES), n_3 = 1.4 x 10^{-7} mol. The maximum amount of photodissociation reaction triggered during the measurement is therefore 2%.

Figure S4 shows the transient absorption spectrum of liposomes **L3** 1.0 ps after the excitation pulse at 400 nm. A negative band ranging from 400 to 500 nm and a weaker positive band from 500 nm onwards are observed. The negative band from 400 to 500 nm coincides with the region of the MLCT absorption band in the steady state absorption spectrum (Figure 1c). Thus this band can be attributed to ground-state bleaching of the ruthenium complex. The broad positive band for λ > 500 nm are attributed to the ^{3}MLCT excited state absorption, as the ^{1}MLCT to ^{3}MLCT intersystem crossing is known to be extremely fast (300 fs time scale).[5] The time evolution of the transient spectrum was best fitted with Glotaran using a model with two exponential decay curves using Glotaran. Two DAS were identified with identical spectra and with lifetimes of 0.17 (53%) and 0.92 ns (47%), hence the average ^{3}MLCT lifetime τ_{Ru} has a value of 0.52 ns.

4.7. Transient absorption in liposomes L23

For liposomes **L23**, i.e. samples containing both **2** and a varying amount of $\mathbf{3}^{2+}$, the time-dependent absorption data was consistently fitted using 5 single exponential decays, similar to as discussed above (Table S4). Each time, it was most satisfactory to fit the decays in the nanosecond regime with a bi-exponential decay. The decay associated spectra for these two components consistently featured the transient spectral characteristics of compound **2**. For calculation of τ with Equation S4, τ_1, τ_2, and τ_5 were irrelevant, so that the reported τ for liposomes **L23** is each time the average of τ_3 and τ_4, i.e. $\tau = \tau_{34}$. The results of these experiments are discussed in the main text.

5. Analysis and quantification of non-radiative energy transfer

5.1. Calculation of energy transfer efficiency E_{ET}

For liposomes **L23**, the energy transfer efficiency (E_{ET}) values were calculated by Equation S6:

$$E_{ET} = 1 - \frac{\tau}{\tau_0} = 1 - \frac{I}{I_0} \quad \textbf{Equation S6}$$

where τ and τ_0 are the amplitude-weighted averages of the excited state lifetime of compound **2** in presence and absence of $\mathbf{3}^{2+}$, respectively, and I and I_0 are the integrated fluorescence intensity of compound **2** in presence and absence of $\mathbf{3}^{2+}$, respectively.[6] Stern-Volmer kinetics are generally applied to photochemical quenching based on collisional quenching, but are to known to may be applicable to FRET systems as well.[7] By rewriting the classical Stern-Volmer equation, see Equation S7,

$$\frac{\tau_0}{\tau} = 1 + K_{SV}[\mathbf{3}] = 1 + k_{SV}\tau_0[\mathbf{3}] \quad \textbf{Equation S7}$$

an expression for E_{ET} is obtained, see Equation S8:

$$E_{ET} = 1 - \frac{1}{1 + K_{SV}[\mathbf{3}]} = \frac{K_{SV}[\mathbf{3}]}{1 + K_{SV}[\mathbf{3}]} \quad \textbf{Equation S8}$$

where K_{SV} is the Stern-Volmer quenching constant (in $L.mol^{-1}$), k_{SV} is the Stern-Volmer rate of quenching ($L.mol^{-1}s^{-1}$), τ_0 is the lifetime of the energy donor without any quencher present, and [**3**] is the bulk concentration of $\mathbf{3}^{2+}$. However, the volume in which the quenching occurs is much smaller than the sample volume, because both compound **2** and $\mathbf{3}^{2+}$ are only located within the membrane. Therefore, [**3**] was substituted with $[\mathbf{3}]_{local}$, i.e. the local concentration of $\mathbf{3}^{2+}$ at the membrane, which is defined by Equation S9:

$$[\mathbf{3}]_{local} = \frac{n_3}{n_{DMPC}V_M} = \frac{x_3}{V_M} \quad \textbf{Equation S9}$$

where n_3 is the number of mol $\mathbf{3}^{2+}$, as calculated by ICP-OES, n_{DMPC} is the number of mol DMPC, V_M is the molar volume of DMPC in lipid bilayers at 293 K (V_M = 0.637 $L.mol^{-1}$),[8] and x_3 is the mol fraction of $\mathbf{3}^{2+}$ in the lipid bilayer. To simplify, we did not account for the volume of DSPE-PEG-2000, **2**, and $\mathbf{3}^{2+}$, because no data was available, and we did not account for the fact that $\mathbf{3}^{2+}$ occupies a volume outside the lipid bilayer as well. Under these assumptions, K_{SV} was found to be 0.32 $L.mol^{-1}$. With τ_0 = 6.2 ns, the value of k_{SV} is 5.2 x 10^7 $L.mol^{-1}s^{-1}$.

5.2. Calculating the theoretical R_0 distance

One of the prerequisites for FRET is to have a good spectral overlap between the donor emission spectrum and acceptor absorption spectrum, as given by the overlap integral J_{DA} (in $M^{-1}cm^{-1}nm^4$) in Equation S10,

$$J_{DA} = \int_0^\infty F_D(\lambda)\varepsilon_A(\lambda)\lambda^4 d\lambda \quad \textbf{Equation S10}$$

where $F_D(\lambda)$ is the area-normalized donor emission spectrum and $\varepsilon_A(\lambda)$ is the molar absorption spectrum of the acceptor (in $L.mol^{-1}cm^{-1}$). J_{DA} = 2.8 x 10^{14} $nm^4M^{-1}cm^{-1}$ for **2** as FRET-donor and $\mathbf{3}^{2+}$ as FRET-acceptor (see Figure 1c). From J_{DA}, the relative orientation factor κ, the refractive index of the medium n (1.334 for PBS buffer), and the fluorescence quantum yield of the donor ϕ_D, the Förster distance R_0 (in Å) can be calculated, for which half the donor molecules decay by FRET, according to Equation S11 below.[6] Assuming κ^2 = 2/3 and using ϕ_D = 0.94 in cyclohexane,[9] R_0 was predicted to be 41 Å.

$$R_0 = 0.211 \times (\kappa^2 n^{-4} \phi_D J_{DA})^{\frac{1}{6}} \quad \textbf{Equation S11}$$

5.3. Fitting lifetime data with a Förster decay model

Besides the use of multi-exponential decays to calculate FRET efficiencies and Stern-Volmer parameters, the time-correlated single photon counting data and transient absorption spectroscopy data were also analysed using a Förster decay model to derive different system parameters. This model has been used before for the analysis of energy transfer from perylene to various transition metal ions in DPPC vesicles.[1, 10] For TCSPC data, Equation S12 was used:

$$I(t) = I_0 e^{-\frac{t}{\tau_0} - 2\gamma\left(\frac{t}{\tau_0}\right)^{1/d}} \qquad \textbf{Equation S12}$$

where I(t) is the time-dependent fluorescence intensity, I_0 is the fluorescence intensity directly after excitation, τ_0 is the FRET donor lifetime in absence [1, 10]of the FRET acceptor, d is the dimensionality of the system (d = 2 and d = 3 for quenching in two and three dimensions, respectively), and γ is defined as [**3**]/C_0, with [**3**] the bulk concentration $\mathbf{3}^{2+}$ (in M) and C_0 the critical acceptor concentration for energy transfer (in M), which is the acceptor concentration needed for 72% energy transfer.[6] In this work, the lifetime data acquired from TCSPC were indeed fitted using the Förster decay model, see Table S2-Table S3. For the fitting, τ_0 was fixed at 6.2 ns. Figure S5 shows a fit of the three-dimensional model (d = 3) on lifetime decay data from TCSPC at 293 K acquired from a liposome sample (**L23**) with 0.5 mol% **2** and 0.9 mol% $\mathbf{3}^{2+}$.

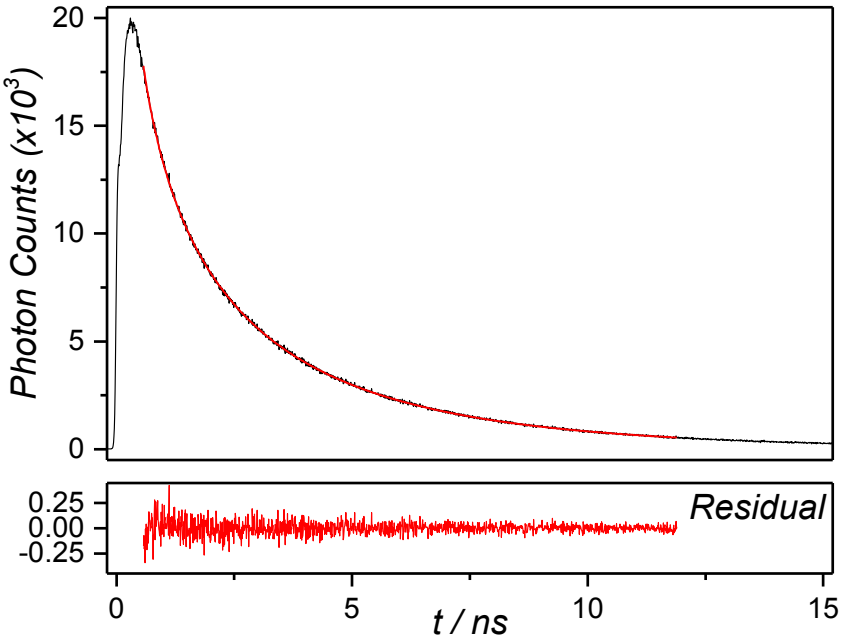

Figure S5. Time-correlated single photon counting decay curve (black) of PEGylated (4 mol%) DMPC liposomes L23, ([DMPC] = 0.2 mM) at 293 K with 0.5 mol% 2 and 0.9 mol% 3^{2+} upon excitation with 440 nm (6 µW laser power, 0.6 pJ/pulse) and collecting emission at 474 nm. The red curve (top) represents a fit of the data according to a 3D FRET model (Equation S12) with d = 3, τ = 6.2 ns, γ = 1.04, with the corresponding residual plot (bottom). The fit has an R^2 value of 0.9995.

In the case of TA spectroscopy data, Equation S12 was modified to Equation S13:

$$\Delta OD(t,\lambda) = \Delta OD(\lambda)_0 \times e^{-\frac{t}{\tau_0} - 2\gamma\left(\frac{t}{\tau_0}\right)^{1/d}} \qquad \textbf{Equation S13}$$

where ΔOD(t,λ) is the observed time-dependent transient absorption spectrum and $\Delta OD(\lambda)_0$ is the transient absorption spectrum at t = 0. It was most convenient to use a kinetic trace at a particular wavelength to fit the

data. Preliminary experiments with TA spectroscopy on **L2** and **L3** alone showed that 400 nm light excites both molecules, but that at 700 nm compound **2** has a major transient absorption peak while there is negligible signal of $\mathbf{3}^{2+}$ (see above). Therefore the kinetic trace at 700 nm was therefore selected for fitting with Equation S13, i.e. λ = 700 nm. Similar to the fitting of TCSPC data, the TA data was indeed fitted using the model (Table S4). Figure S6 shows a fit of the three-dimensional model (d = 3) on lifetime decay data from TA at 293 K acquired from a liposome sample **L23** with 0.5 mol% **2** and 0.8 mol% $\mathbf{3}^{2+}$.

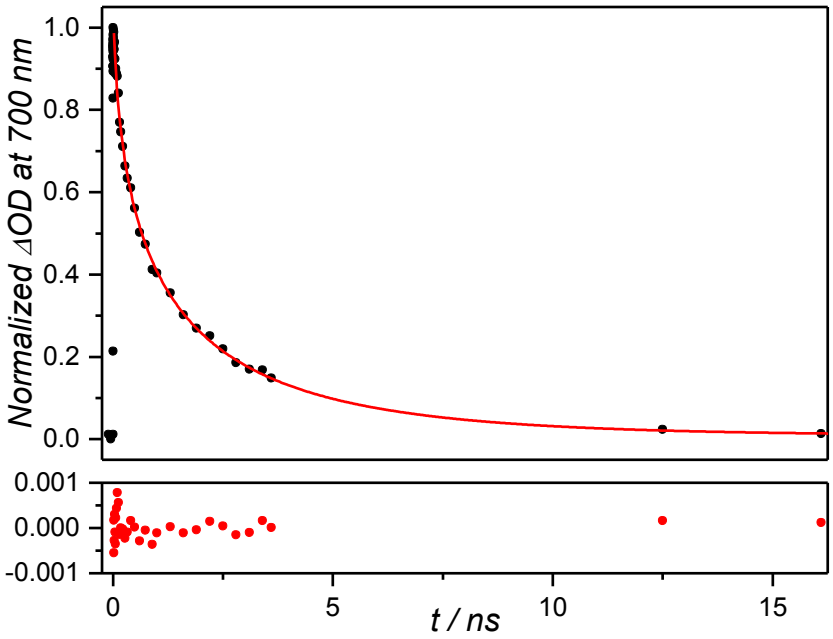

Figure S6. Transient absorption decay curve at 700 nm (black) of PEGylated (4 mol%) DMPC liposomes L23 ([DMPC] = 20 mM) at 293 K with 0.5 mol% 2 and 0.8 mol% 3^{2+} upon excitation with 400 nm (20-60 nJ/pulse, 1 KHz repetition rate). The red curve (top) represents a fit of the data according to a 3D FRET model (Equation S12) with d = 3, τ = 6.0 ns, γ = 0.99, with the corresponding residual plot (bottom). The fit has a R^2 value of 0.997.

The fitting parameters of the Förster three-dimensional decay model for both TCSPC and TA data, listed in Table S2-Table S4, show that for greater concentration of $\mathbf{3}^{2+}$, higher values of γ are obtained. In general, a three-dimensional model fitted the data better than a two-dimensional model, as the 3D model produced fits with X^2 values closer to 1. This agrees with the work of Holmes *et al.*[1, 10]

5.4. Calculating the experimental R_0 distance

The critical acceptor concentration C_0 (in M) is related to R_0 (in dm) by Equation S14:

$$C_0 = \frac{3}{2\pi^{\frac{3}{2}} N_A R_0^3} \qquad \textbf{Equation S14}$$

so that a plot of γ versus [**3**] provided a straight line, of which the slope $1/C_0$ was used to evaluate R_0 (in dm), see Figure S7. Again, [**3**] was substituted with $[\mathbf{3}]_{local}$ (see Equation S9). In such conditions, R_0 was calculated to be 29 Å.

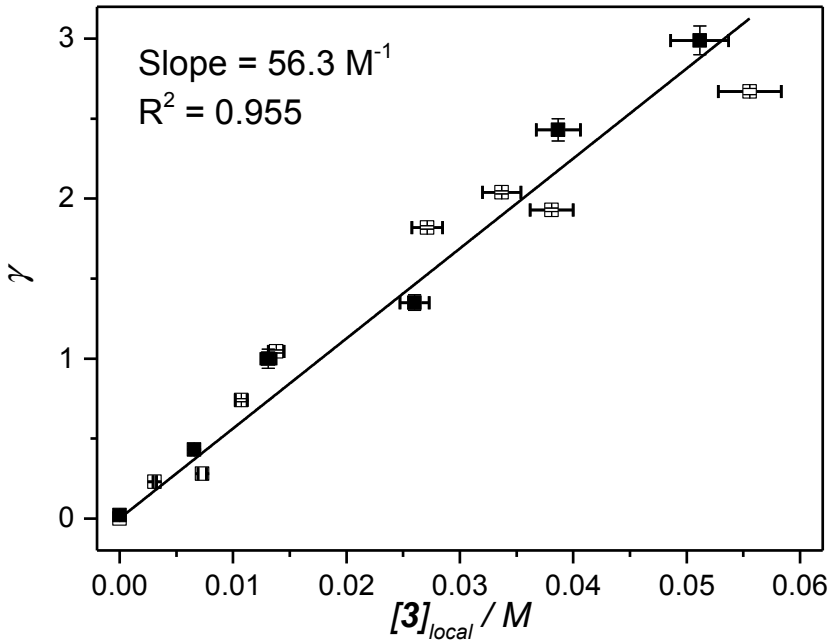

Figure S7. Plot of γ at 293 K, as determined from transient absorption data (black filled squares) or from time-correlated single photon counting data (empty squares), as a function of the local concentration of 3^{2+}, as defined by Equation S9, in the lipid bilayer of PEGylated DMPC liposomes as determined by ICP-OES. Horizontal error bars represent 5% instrumental error from ICP-OES. Vertical error bars represent the fitting error of Equation S12 on the data. The black line represents the best linear fit from the origin through the two combined data sets, and has a slope of 56.3 M^{-1} with R^2 = 0.955.

6. Photodissociation experiments using red light

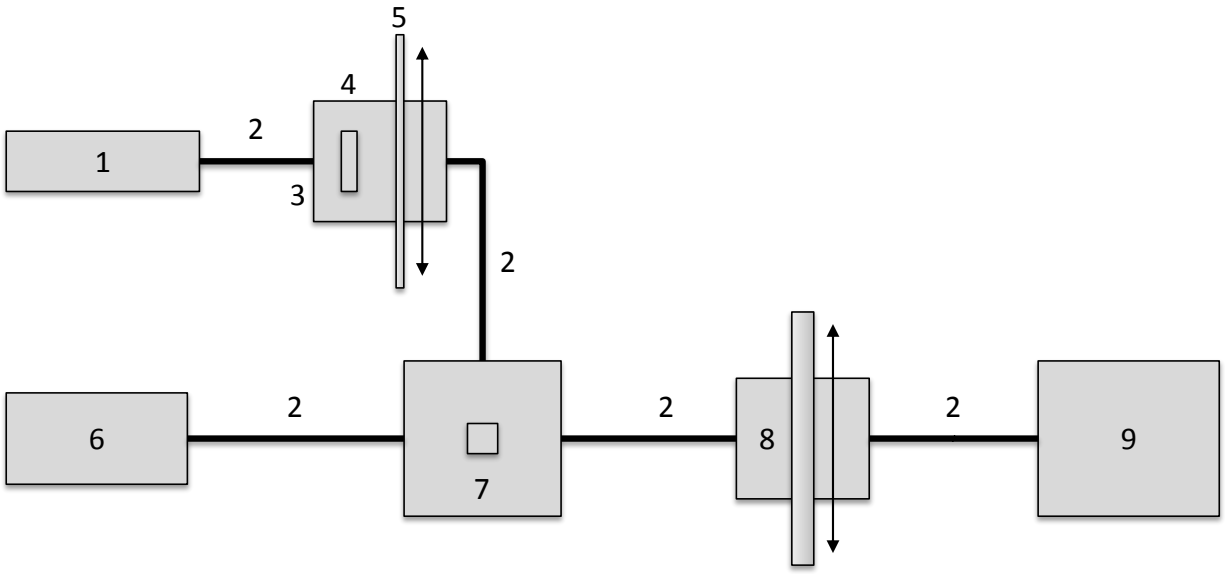

Figure S8. Setup used for photosubstitution experiments using red light. Legend: (1) 630 nm laser source, (2) optical fibres, (3) filter holder, (4) 630 nm band pass filter, (5) variable neutral density filter that can be installed or removed, (6) halogen-deuterium light source for UV-Vis absorption spectroscopy, (7) temperature controlled cuvette holder, (8) variable filter holder, and (9) CCD spectrometer.

7. Determination of quantum yield of upconversion

7.1. Experimental setup

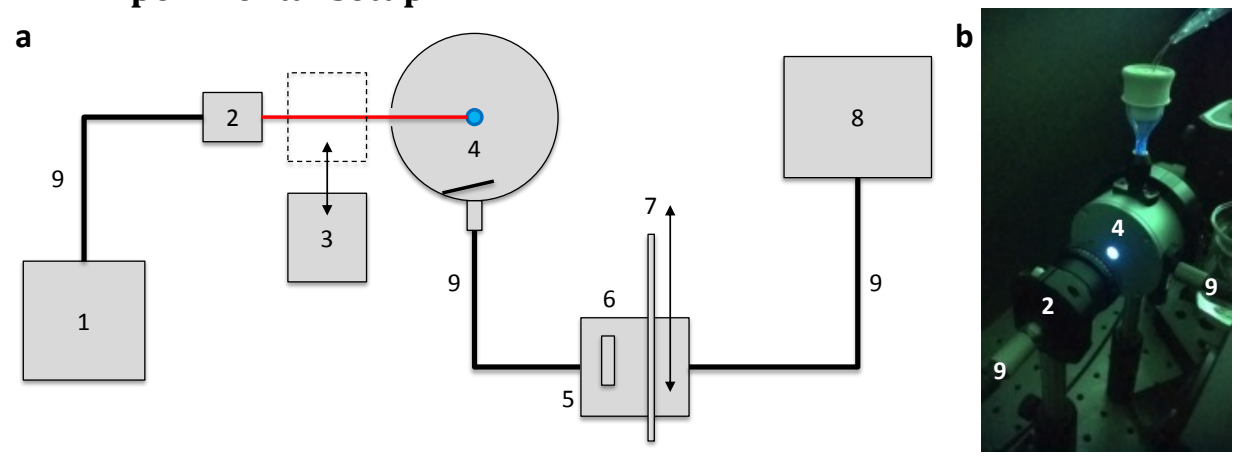

Figure S9. Setup used for absolute quantum yield measurements. a) Schematic representation; (1) laser source, (2) collimating lens, 630 nm band pass filter, and mechanical iris (3) power meter adjustable in position, (4) integrating sphere with sample tube in the centre, (5) filter holder, (6) notch filter that can be installed or removed, (7) variable neutral density filter that can be installed or removed, (8) CCD spectrometer, (9) optical fibres. b) Picture of the integrating sphere while irradiating a sample with 630 nm light, while holding a 630 nm notch filter in front of the camera to block the red-light scatter. The blue light originates from the upconversion in the sample.

An integrating sphere setup was used for determining the quantum yield of upconversion (Figure S9). The excitation source was a clinical grade Diomed 630 nm PDT laser. This laser only operates with an optical fibre connection, and was therefore connected with a FC-UV200-2 optical fibre (Avantes, Apeldoorn, The Netherlands) to a collimating lens, after which the light passed a 630 nm band pass filter and a mechanical iris to produce a ca. 2 mm beam. The excitation power was measured using a S310C thermal sensor connected to a PM100USB power meter (Thorlabs, Dachau/Munich, Germany). An AvaSphere-30-IRRAD integrating sphere, customized with a sample holder and an extra aperture, and an AvaSpec-ULS2048L StarLine CCD spectrometer were purchased from Avantes. The integrating sphere and spectrometer were calibrated so that the observed intensities are expressed with the dimension of a photon flux (photon.s^{-1}.m^{-2}, where the surface is that of the entrance aperture in the integrating sphere). The filter holder was fabricated by our own mechanical department, and held a NDL-25C-4 variable neutral density filter (Thorlabs), or an OD4 575 nm short pass filter (Edmund Optics, York, United Kingdom, part no. 84-709). The FC-UVxxx-2 (xxx = 200, 400, 600) optical fibres with 200-600 µm diameter were purchased from Avantes and were suitable for the UV-Vis range (200-800 nm). Spectra were recorded with Avasoft software from Avantes (The Netherlands) and further processed with Microsoft Office Excel 2010 and Origin Pro software.

7.2. Procedure for determining the quantum yield of upconversion

The quantum yield of upconversion (Φ_{uc}) is defined by Equation S15:

$$\Phi_{UC} = \frac{\text{number of upconverted photons}}{\text{number of low-energy photons absorbed}} = \frac{q_{p-em}}{q_{p-abs}} \quad \textbf{Equation S15}$$

where $q_{p\text{-}em}$ is the emission photon flux of the singlet annihilator species (in photons.s^{-1}) and $q_{p\text{-}abs}$ is the photon flux absorbed by the sensitizer species (in photons.s^{-1}). Note that for TTA-UC quantum yields, it is common to multiply Φ_{uc} by 2, because of the fact that TTA-UC intrinsically has a maximum quantum yield of 50% and thus must be scaled to attain a maximum value of 100%. In this work, we do not use such a misleading scaling factor. Φ_{uc} can be calculated by Equation S16:

$$\Phi_{UC} = \frac{\int_{\lambda_1}^{\lambda_2} I_{annihilator}(\lambda)d\lambda}{q_{p-abs}} \quad \textbf{Equation S16}$$

where $I_{annihilator}(\lambda)$ is the spectral luminescence intensity (in photons.s^{-1}.nm^{-1}) of the annihilator species, λ_1 and λ_2 are the low- and high-wavelength boundaries, respectively, of the upconverted annihilator emission spectrum. $q_{p\text{-}abs}$ is determined by subtracting the spectral light intensity of the excitation source that has passed through the sample ($I_{exc\text{-}sample}$, in photons.s^{-1}.nm^{-1}) from the spectral light intensity of the excitation source that has passed through a blank sample ($I_{exc\text{-}blank}$, in photons.s^{-1}.nm^{-1}), and by integrating over the excitation wavelength range λ_3 to λ_4, see Equation S17. The blank sample resembled the upconverting sample in all ways, except that it did not contain any sensitizer, and thus did not absorb at the excitation wavelength.

$$q_{p-abs} = \int_{\lambda_3}^{\lambda_4} I_{exc-blank}(\lambda) - I_{exc-sample}(\lambda)d\lambda \quad \textbf{Equation S17}$$

Equation S16 can then be expressed as Equation S18:

$$\Phi_{UC} = \frac{\int_{\lambda_1}^{\lambda_2} I_{annihilator}(\lambda)d\lambda}{\int_{\lambda_3}^{\lambda_4} I_{exc-blank}(\lambda) - I_{exc-sample}(\lambda)d\lambda} \quad \textbf{Equation S18}$$

The spectrometer and the integrating sphere were calibrated so that the observed intensities are directly proportional to the photon flux, i.e. $I(\lambda) \propto [\text{mol of photons}.\,s^{-1}.\,nm^{-1}]$. Therefore, integrating these values over the relevant wavelength regions gave directly the flux of photons arriving at the spectrometer.

Because the intensity of the upconverted light is relatively low compared to that of the exciting laser source the absorption and emission of the sample cannot be measured at the same time. In other words, the laser light saturates the spectrometer, which prevents upconversion to be measured. To circumvent this problem, the absorption was measured using a variable neutral density filter with known attenuation (typically F_{attn}~0.01, *i.e.*, ~99% attenuation). This filter was placed between the integrating sphere and the spectrometer to measure the absorbed photon flux, whereas it was replaced for the measurement of the upconverted emission by an OD4 short pass filter (<575 nm) to remove the excitation wavelength. Thus, Equation S18 was changed into Equation S19. The attenuation factor F_{attn} was assumed to be constant over the wavelength range of the laser excitation. Additionally, because the sample was relatively concentrated so that enough red light was absorbed to have an accurate value of $q_{p\text{-}abs}$, a correction was required for $I_{annihilator}$ for the secondary inner-filter effect, due to reabsorption of the emission around 450 nm. To this end, the upconversion emission spectrum was recorded under

highly diluted conditions in the temperature controlled cuvette holder setup (see experimental section in the main text) and this spectrum was scaled at 474 nm (i.e. the second emission peak of perylene, which is not reabsorbed) to match the photon flux value at 474 nm of $I_{annihilator}$. This corrected spectrum was called $I_{annihilator\text{-}corr}$. Finally, although at the first order the notch or short pass filter was assumed to only block the laser signal from reaching the spectrometer, in reality there was a small reduction of transmission for wavelengths situated in the upconversion range as well. This filtering can be corrected when calculating Φ_{uc} by dividing the upconversion luminescence intensity by the transmission curve $T(\lambda)$ of the notch or short pass filter in the wavelength range of the upconverted light. The corrected equation for Φ_{uc} became Equation S19:

$$\Phi_{UC} = \frac{\int_{\lambda_1}^{\lambda_2} \left(\frac{I_{annihilator-corr}(\lambda)}{T(\lambda)} \right) d\lambda}{\int_{\lambda_3}^{\lambda_4} \frac{I_{exc-blank}(\lambda) - I_{exc-sample}(\lambda)}{F_{attn}} d\lambda} \equiv \frac{q_{p-em}}{q_{p-abs}} \qquad \textbf{Equation S19}$$

Because the integrating sphere setup did not feature temperature control, Φ_{UC} at 310 K was estimated from measuring the upconversion emission under highly diluted conditions in the temperature controlled cuvette holder setup at 293 K and at 310 K (see experimental section in the main text) and scaling Φ_{UC} at 293 K with the ratio of the upconversion emission at 293 K and 310 K by using Equation S20:

$$\Phi_{UC}^{310\,K} = \Phi_{UC}^{293\,K} * \frac{\int_{\lambda_1}^{\lambda_2} I_{annihilator}^{310\,K}(\lambda) d\lambda}{\int_{\lambda_1}^{\lambda_2} I_{annihilator}^{293\,K}(\lambda) d\lambda} \qquad \textbf{Equation S20}$$

The boundary wavelengths that were used for determining Φ_{uc} given in the main text, as well as the measured values for $q_{p\text{-}em}$ and $q_{p\text{-}abs}$ at 293 K, are given in Table S5.

Table S5. Values used for Φ_{uc} determination at 293 K.

	λ1 (nm)	λ2 (nm)	λ3 (nm)	λ4 (nm)	$q_{p\text{-}em}$ (nmol photons.s^{-1})	$q_{p\text{-}abs}$ (nmol photons.s^{-1})	Φ_{uc}
L12	400	575	615	645	0.705	30.0	0.024

For each measurement, two liposome samples were prepared: one blank sample, containing the annihilator (**2**) but deprived of sensitizer (**1**), i.e. liposomes **L2**, and one with the upconversion couple (**1** + **2**), i.e. liposomes **L12**. Since the concentration of the sensitizer is very small compared to the other liposome constituents ([**1**] ≤ 0.05 mol%), we assume that removal of the sensitizer from the lipid mixture did not influence the physical properties of the liposomes (membrane fluidity, scattering properties of the sample, or others). The upconverting sample **L12** or the blank sample **L2** was loaded into specially designed measurement tubes that were made of a quartz EPR-tube bottom (± 7 cm length) fused to a NS-14 glass connector (± 2 cm length), at the top of which a septum was adapted. The tube fit precisely a hole made in the integrating sphere, and reached the centre of the sphere, where it was hit by the excitation laser beam. Deoxygenation of the sample was performed in a separate ice-cooled, pear-shaped flask, by bubbling the sample with argon for at least 30 minutes with a rate of ~2 bubbles per second. The degassed sample was then transferred in the measurement tube by cannulation in the strict absence of oxygen. Degassing in the tube was found to be impossible due to foam formation.

8. Definition and calculation of the total efficiency of TTA-UC, FRET and photodissociation

When TTA-UC and FRET are combined within the same membrane to realize the photochemical conversion of $\mathbf{3}^{2+}$ to $\mathbf{4}^{2+}$, the relevant photophysical and photochemical steps are

$$^1PS \xrightarrow{h\nu} {}^1PS^*$$

$$^1PS^* \xrightarrow{k_{ISC}} {}^3PS^*$$

$$^3PS^* + {}^1A \xrightarrow{k_{TTET}} {}^1PS + {}^3A^*$$

$$2\ {}^3A^* \xrightarrow{k_{TTA}} {}^1A + {}^1A^*$$

$$^1A^* + {}^1\mathbf{3}^{2+} \xrightarrow{k_{ET}} {}^1A + {}^1\mathbf{3}^{2+*}$$

$$^1\mathbf{3}^{2+*} \xrightarrow{k_{photosubstitution}} {}^1\mathbf{4}^{2+}$$

where for clarity purposes PS is the photosensitizer (**1**), and A is the annihilator (**2**), ISC means intersystem crossing, TTET means triplet-triplet energy transfer, TTA means triplet-triplet annihilation, and ET means non-radiative energy transfer. The rate of reaction is then defined by Equation S21,

$$r = -\frac{dn_{\mathbf{3}^{2+}}}{dt} = \left|\frac{dn\ {}^1{}_{PS}}{dt}\right|_{created} \phi_{ISC}\phi_{TETT}\phi_{TTA}E_{ET}\phi_{Ru} \qquad \textbf{Equation S21}$$

where $\left|\frac{dn\ {}^1{}_{PS}}{dt}\right|_{created}$ is the rate of singlet state photosensitizer generated, ϕ_{ISC} is the QY of ISC of the photosensitizer, ϕ_{TETT} is the QY of TTET, ϕ_{TTA} is the QY of TTA, E_{ET} is the energy transfer efficiency as defined in Equation S8, and ϕ_{Ru} is the quantum yield of photosubstitution in absence of **1** and **2**, measured under blue light irradiation. The rate of singlet state photosensitizer generated is further defined by Equation S22:

$$\left|\frac{dn\ {}^1{}_{PS}}{dt}\right|_{created} = \Phi_{630}(1 - 10^{-A_{630}}) \qquad \textbf{Equation S22}$$

where Φ_{630} is the photon flux at 630 nm (einstein.s^{-1}) and A_{630} is the absorbance of the photosensitizer at 630 nm. In addition, similarly to Equation S8, the efficiency of non-radiative energy transfer, E_{ET}, is given by Equation S23:

$$E_{ET} = 1 - \frac{1}{1 + K_{SV} * [\mathbf{3}]_{local}} = \frac{K_{SV}[\mathbf{3}]_{local}}{1 + K_{SV}[\mathbf{3}]_{local}} \qquad \textbf{Equation S23}$$

where $[\mathbf{3}]_{local}$ is the local concentration of $\mathbf{3}^{2+}$ in the membrane, defined by Equation S9 ($[\mathbf{3}]_{local} = \frac{n_{\mathbf{3}}}{n_{DMPC}V_M}$), and K_{SV} is the Stern-Volmer constant (L.mol^{-1}) for the quenching of ^{1}A* by $\mathbf{3}^{2+}$ in the lipid membrane. The quantum yield of TTA-UC is given by Equation S24:

$$\phi_{ISC}\phi_{TETT}\phi_{TTA} = \phi_{TTA-UC} \qquad \textbf{Equation S24}$$

Thus Equation S21 becomes Equation S25:

$$r = -\frac{dn_{\mathbf{3}}}{dt} = \Phi_{630}(1 - 10^{-A_{630}})\phi_{TTA-UC}\frac{K_{SV}[\mathbf{3}]_{local}}{1 + K_{SV}[\mathbf{3}]_{local}}\phi_{Ru} \qquad \textbf{Equation S25}$$

Equation S25 shows that the rate of the photosubstitution reaction depends on the local concentration of $\mathbf{3}^{2+}$ and a non-zero order reaction rate can be expected. Realizing that $K_{SV}[\mathbf{3}]_{local} << 1$, and that therefore E_{ET} can be approximated with $K_{SV}[\mathbf{3}]_{local} \equiv K_{SV}\frac{n_{\mathbf{3}}}{n_{DMPC}V_M}$, Equation S25 simplifies to Equation S26:

$$r = -\frac{dn_3}{dt} = \Phi_{630}(1 - 10^{-A_{630}})\phi_{TTA-UC}K_{SV}\frac{n_{\mathbf{3}}}{n_{DMPC}V_M}\phi_{Ru} \qquad \textbf{Equation S26}$$

Integrating Equation S26 yields a first-order expression for $n_{\mathbf{3}}(t)$:

$$n_{\mathbf{3}}(t) = n_{\mathbf{3}}(0) * e^{-kt} \qquad \textbf{Equation S27}$$

where k is given by Equation S28:

$$k = \frac{\Phi_{630}}{n_{DMPC}V_M}(1 - 10^{-A_{630}})\phi_{TTA-UC}K_{SV}\phi_{Ru} \qquad \textbf{Equation S28}$$

The total efficiency of TTA-UC, FRET, and photodissociation of $\mathbf{3}^{2+}$ in liposomes **L123** is defined by Equation S29:

$$E_{total} = \phi_{TTA-UC}E_{ET}\phi_{Ru} \approx \phi_{TTA-UC}K_{SV}\frac{n_{\mathbf{3}}}{n_{DMPC}V_M}\phi_{Ru} \qquad \textbf{Equation S29}$$

For t = 0 – 45 min, i.e. when E_{ET} is more or less constant, E_{total} can be experimentally determined from a plot of the amount of mol of $\mathbf{3}^{2+}$ as a function of the amount of absorbed photons, i.e. $\Phi_{630} * (1 - 10^{-A_{630}}) * t$, see Figure S10. Φ_{630} was estimated from measuring the optical power (120 mW at 630 nm, i.e. 0.632 µeinstein.s^{-1}) and A_{630} was 0.025. Note that at t = 0, mostly **1** absorbs at 630 nm. Some bleaching of **1** was observed during the reaction (see Figure 2b), but it was neglected in this calculation. Therefore, the amount of absorbed photons per unit time was considered to be constant. E_{total} at t = 0 can be evaluated from the slope at t = 0 of the single exponential fit curve of the evolution of $n_{\mathbf{3}}$ versus the amount of red photons absorbed since t = 0 (see Figure S10). From this, a value of 0.027% was determined.

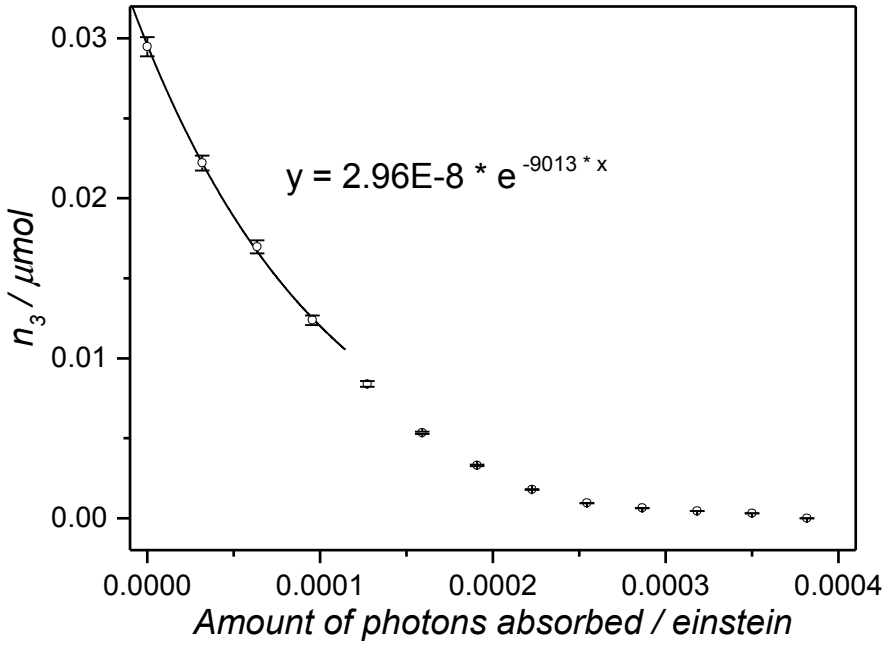

Figure S10. Plot of n_3 as a function of the amount of photons absorbed during the photodissociation experiment with red light of L123. The black line represents a single exponential fit for the first 45 min of irradiation.

The amount of mol $\mathbf{3}^{2+}$ was determined from the UV-VIS absorbance data at 490 nm by accounting for the contributions of both $\mathbf{3}^{2+}$ and $\mathbf{4}^{2+}$ to the absorption at this wavelength, as explained here. The total absorbance at 490 nm is given by Equation S30:

$$A^{490} = \varepsilon_{\mathbf{3}}^{490} \times l \times [\mathbf{3}] + \varepsilon_{\mathbf{4}}^{490} \times l \times [\mathbf{4}] \qquad \textbf{Equation S30}$$

where $\varepsilon_{\mathbf{3}}^{490}$ is the molar absorption coefficient of $\mathbf{3}^{2+}$ at 490 nm (3760 $M^{-1}cm^{-1}$ in $CHCl_3$), [**3**] is the bulk concentration of $\mathbf{3}^{2+}$, $\varepsilon_{\mathbf{4}}^{490}$ is the molar absorption coefficient of $\mathbf{4}^{2+}$ at 490 nm (8690 $M^{-1}cm^{-1}$ in H_2O), [**4**] is the bulk concentration of $\mathbf{4}^{2+}$, and l is the cuvette path length (i.e. 1 cm). At t = ∞, the photoreaction is complete and no more $\mathbf{3}^{2+}$ is present, which means that

$$A_{\infty}^{490} = \varepsilon_{\mathbf{4}}^{490} \times l \times [\mathbf{3}]_0 \qquad \textbf{Equation S31}$$

By replacing [**4**] with $[\mathbf{3}]_0 - [\mathbf{3}]$ in Equation S30, [**3**] can be expressed as a function of A^{490} in Equation S32:

$$[\mathbf{3}] = \frac{A^{490} - A_{\infty}^{490}}{\varepsilon_{\mathbf{3}}^{490} \times l - \varepsilon_{\mathbf{4}}^{490} \times l} \qquad \textbf{Equation S32}$$

Finally, the amount of mol $\mathbf{3}^{2+}$ is obtained by multiplying with the volume in the cuvette (V, i.e. 1.5 ml), see Equation S33:

$$n_{\mathbf{3}} = V * \frac{A^{490} - A_{\infty}^{490}}{\varepsilon_{\mathbf{3}}^{490} - \varepsilon_{\mathbf{4}}^{490}} \qquad \textbf{Equation S33}$$

At t = 0, the value for n_3 ($2.95 \times 10^{-8} \pm 0.06 \times 10^{-8}$ mol) was very comparable with the value for n_3 determined by ICP-OES ($2.82 \times 10^{-8} \pm 0.01 \times 10^{-8}$) , which confirms the validity of this approach.

9. Power dependency of TTA-UC and determination of I_{TH}

Warning: All data in section 9 were published recently[11] and are repeated here for convenience to the reader.

Luminescence emission spectra of **L12** were recorded at various excitation powers from 1 to 40 mW so that the excitation intensity (P) was 8 to 318 mW.cm^{-2} (4 mm laser beam diameter). The samples were placed in a Hellma 101-OS macro fluorescence cuvette (2.25 mL, [lipid] = 1.0 mM) and thermally equilibrated at 298 K before measurement in the same setup as described in the main text (see experimental section, "Photodissociation experiments with red light"). In this case, the spectrum was visualized with only a Thorlabs NF-633 notch filter in between the sample and the detector.

The recorded spectra were integrated from 420 to 575 nm to obtain the integrated upconversion luminescence intensity (I_{UC}), which was then plotted in a double logarithmic plot as a function of the excitation intensity (Figure S11). The low power (≤ 40 mW.cm^{-2}) and high power (≥ 120 mW.cm^{-2}) regimes were consistently fitted with slopes around 1 and 2, respectively, which shows the typical two-regime power dependency of TTA-UC. The intersection of these straight lines represents the intensity threshold (I_{th}) at which the power dependency changes from quadratic to linear. I_{th} was found to be 50 mW.cm^{-2} for TTA upconversion in liposomes **L12**.

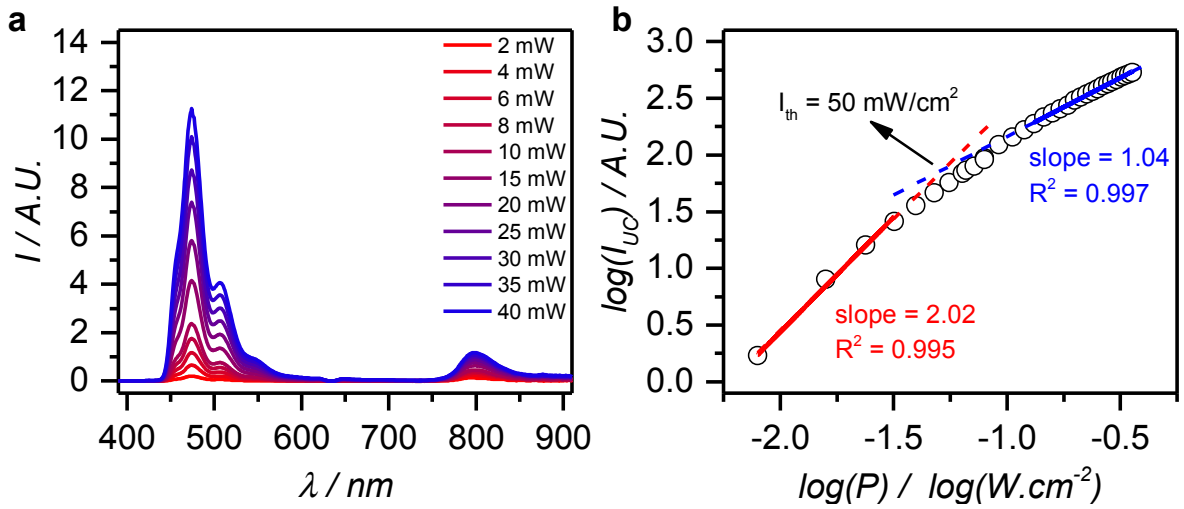

Figure S11. a) Luminescence emission spectra of L12 at various excitation intensities. b) Double logarithmic plot of the upconversion luminescence intensity (I_{UC}) of L12, integrated from 420 to 575 nm, as a function of the excitation intensity P (in W.cm^2). The low power regime was fitted with a straight line with slope 2.02 (R^2 = 0.995) (red solid line), and the high power regime was fitted with a straight line with slope 1.04 (R^2 = 0.997) (blue solid lines). From the intersection of the extrapolated fits (red and blue dashed lines), the intensity threshold (I_{th}) was found to be 50 mW.cm^{-2}. Irradiation conditions: [lipid] = 1.0 mM, T = 298 K, laser beam diameter 4 mM.

10. Photodissociation experiments with lower red-light intensities

Irradiation experiments on liposomes **L123** were repeated with three different red light intensities of 30, 60, and 120 mW (0.24, 0.48, and 0.95 W.cm^{-2}, respectively). The course of the reaction was monitored by UV-Vis absorption spectroscopy following the absorbance of the aqua photoproduct at 490 nm (Figure S12). As expected, a decrease in reaction rate was observed for lower irradiation intensities (Figure S12d). To determine the total efficiency of the system (E_{total}, see section 8), the amount of ruthenium (n_3) was plotted versus the amount Q of photons absorbed since t=0 (Figure S13). E_{total} was calculated from the exponential fit of the data by multiplying the exponent with the amplitude, yielding values of 0.026% for 0.24 W.cm^{-2}, 0.024% for 0.48 W.cm^{-2}, and 0.019% for 0.95 W.cm^{-2}. The somewhat lower quantum yield for the experiment using 0.95 W.cm^{-2} irradiation is attributed to some bleaching of the photosensitizer (**1**) in this particular experiment (compare A_{630} at t = 180 between the three individual experiments in Figure S12). The real amount of photons absorbed by **1** is therefore lower (i.e. the real quantum yield is higher), but the data is not corrected for this effect. Overall, all three efficiencies values E_{total} were found very similar to that given in the main text (0.027% for 0.95 W.cm^{-2} red light irradiation), so it can be concluded that the quantum efficiency of red light-induced photosubstitution in **L123** is unaffected by light intensity and this range of intensities.

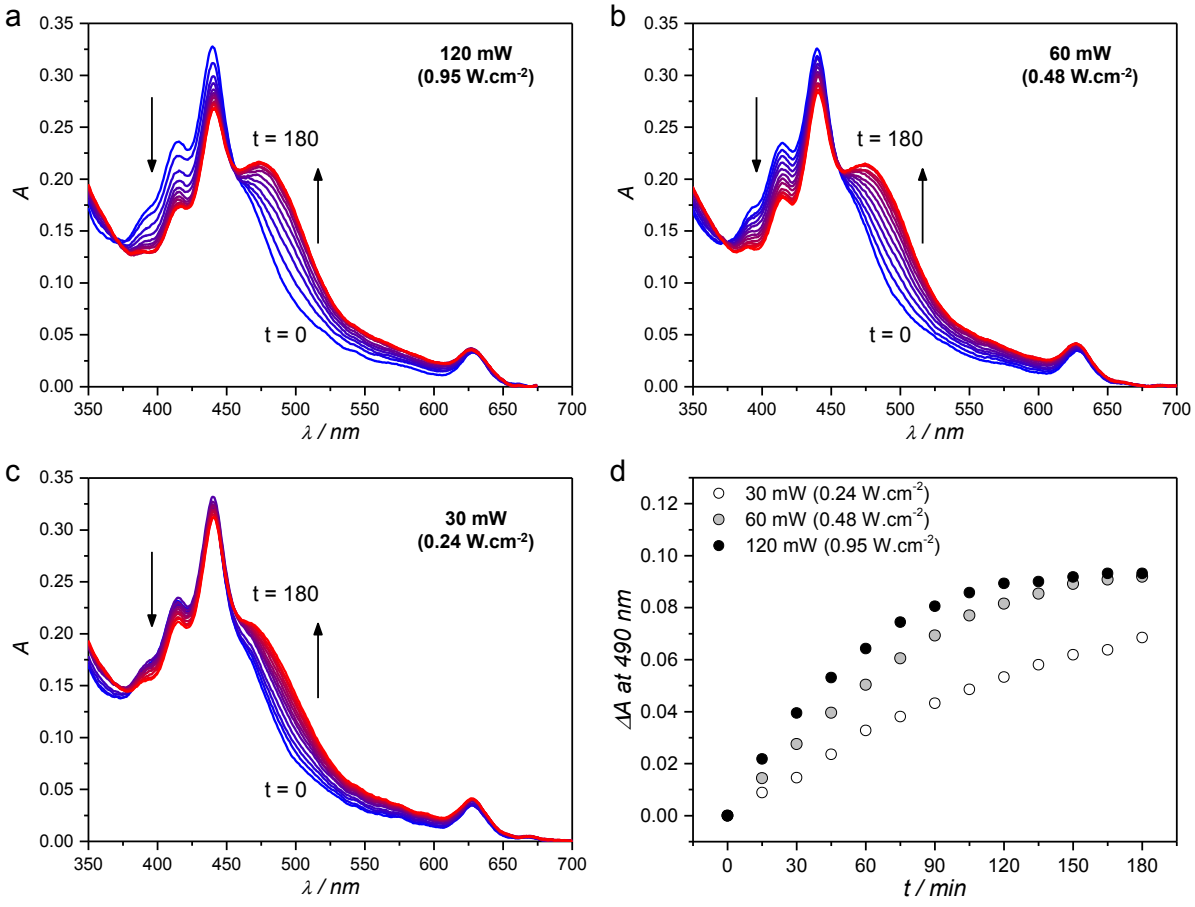

Figure S12. Absorption spectra of liposomes L123 during red light irradiation (630 nm) with (a) 30 mW (0.24 W.cm^{-2}), (b) 60 mW (0.48 W.cm^{-2}), and (c) 120 mW (0.95 W.cm^{-2}). Blue line: spectrum at t = 0; red line: spectrum at t = 180 minutes; other spectra measured every 15 minutes. d) Difference in absorbance at 490 nm, after baseline correction, during red-light irradiation of L123 with 30 mW (white), 60 mW (grey), or 120 mW (black). T = 310 K, sample volume 1.5 ml, 8% of sample volume simultaneously irradiated. A single L123 liposome stock dispersion was used in these experiments and diluted with PBS buffer prior to measurement so that every time [1] = 0.25 µM, and [2] = 2.5 µM.

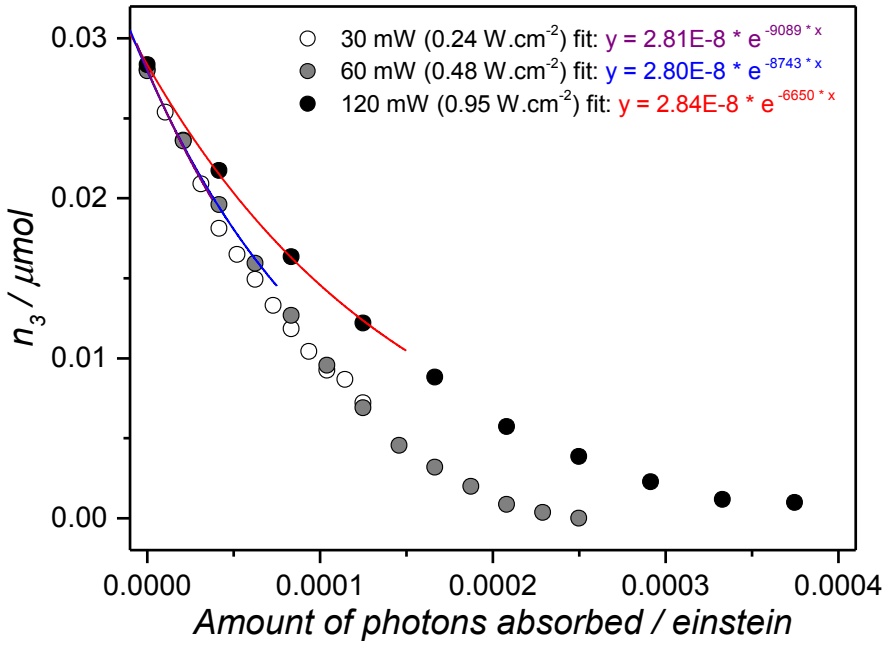

Figure S13. Evolution of the number of mol of 3^{2+} (n_3) as a function of the amount of red photons absorbed since t=0 for liposome sample L123 irradiated with 30 mW (0.24 W.cm^{-2} white circles, purple fit curve), 60 mW (0.48 W.cm^{-2}, grey circles, blue fit curve), or 120 mW (0.95 W.cm^{-2}, black circles, red fit curve). The fit lines represent single exponential fits for the first 45 min of irradiation for each dataset. The lower slope for the 120 mW experiment is attributed to more bleaching of the photosensitizer during irradiation.

11. References

1. A. S. Holmes, D. J. S. Birch and T. Salthammer, *J Fluoresc*, 1993, **3**, 77-84.
2. S. L. Joris J. Snellenburg, Ralf Seger, Katharine M. Mullen, Ivo H. M. van Stokkum, *Journal of Statistical Software*, 2012, **49**, 1-22.
3. Y. H. Meyer and P. Plaza, *Chem. Phys.*, 1995, **200**, 235-243.
4. S. Bonnet, B. Limburg, J. D. Meeldijk, R. J. M. K. Gebbink and J. A. Killian, *J. Am. Chem. Soc.*, 2010, **133**, 252-261.
5. N. H. Damrauer, G. Cerullo, A. Yeh, T. R. Boussie, C. V. Shank and J. K. McCusker, *Science*, 1997, **275**, 54-57.
6. J. R. Lakowicz, *Principles of Fluorescence Spectroscopy*, Springer Science+Business Media, LLC, New York, NY, USA, 3rd edn., 2006.
7. J. T. Buboltz, C. Bwalya, S. Reyes and D. Kamburov, *The Journal of Chemical Physics*, 2007, **127**, 215101.
8. D. Marsh, *Handbook of Lipid Bilayers*, Taylor & Francis Group, LLC, Boca Raton, FL, USA, 2nd edn., 2013.
9. I. B. Berlman, *Handbook of fluorescence spectra of aromatic molecules*, Academic Press, New York, NY, USA, 2nd edn., 1971.
10. A. S. Holmes, K. Suhling and D. J. S. Birch, *Biophysical Chemistry*, 1993, **48**, 193-204.
11. S. H. C. Askes, N. L. Mora, R. Harkes, R. I. Koning, B. Koster, T. Schmidt, A. Kros and S. Bonnet, *Chem. Commun.*, 2015, 9137-9140.